中國機械工程學刊第四十六卷第四期第 407~421 頁(民國一百一十四年)
Journal of the Chinese Society of Mechanical Engineers, Vol.46, No.4, pp407~421 (2025)

Analysis of Belt Deviation Characteristics of Conveyor Belt in Belt Storage Units Based on Lateral Multi-Body Dynamics Modelling

Xiao-Xia Sun* and Jian Wu**

Keywords：Telescopic belt conveyor, Belt storage units, Lateral multi-body dynamics, Lateral deviation characteristics.

ABSTRACT

The research on the causes and characteristics of belt deviation in the belt storage units of a telescopic belt conveyors is of significant importance for designing corresponding correction systems to enhance the operational stability and lifespan of the conveyor. This paper analyzes the normal, tangential, and lateral contact forces and restoring forces between the conveyor belt, pulleys, and idlers. Using a multi-body dynamics (MBD) method, a lateral MBD model of the multi-layer, multi-directional conveyor belt in the belt storage units is established, and simulation analyses are conducted to investigate its deviation characteristics. The results indicate that when the conveyor belt approaches or passes over a pulley with a deflection angle, it exhibits deviation movement. When the take-up pulleys have an in-plane and out-of-plane deflection angle, the maximum deviation of the conveyor belt occurs at the take-up pulley 3 and take-up pulley 2, respectively. Furthermore, the deviation of the conveyor belt is positively correlated with the deflection angle and the center distance of the pulleys. After deviating, when the conveyor belt passes through a take-up pulley or idler with an in-plane deflection angle, a resetting phenomenon occurs, thereby reducing the amount of deviation.

INTRODUCTION

The telescopic belt conveyors is an important piece of equipment for transporting raw coal underground in coal mines and it plays a crucial role in the coal mining industry. The proper alignment of the conveyor belt is a necessary condition for the safe operation of the telescopic belt conveyor. However, due to the complex working environment, the conveyor belt often experiences deviation, especially in the case of multi-layer and multi-directional belt arrangements within the storage units, where the issue is more severe and difficult to manage. There are primarily two reasons for the deviation: First, during the process of the conveyor belt retraction and extension, a gap exists between the edge of the take-up pulleys wheel and the track. When the take-up pulleys move, it can easily become misaligned, causing the take-up pulleys on the trolley to experience an in-plane deflection angle β_H (Figure 1a), the pulley is deflected in the XZ plane about the center point of the axis. Second, geological changes can result in uneven ground surfaces during use, leading to an out-of-plane deflection angle β_V (Fig. 1b), the pulley is deflected in the YZ plane about the center point of the axis. To study the correction system for belt deviation in the belt storage units, it is essential first to understand the characteristics of multi-layer, multi-directional conveyor belts within the storage units.

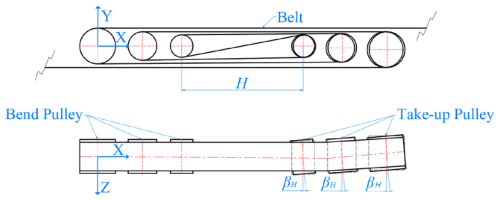

(a) In-plane deflection angle β_H

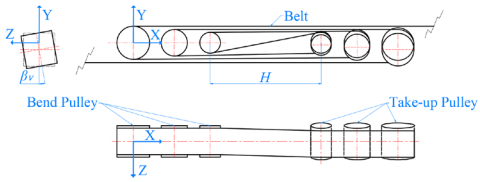

(b) Out-of-plane deflection angle β_V

Fig 1. Deflection angle of the take-up pulleys in the belt storage units.

Many scholars have studied the problem belt

Paper Received July, 2024. Revised January, 2025. Accepted February, 2025. Author for Correspondence: Jian Wu
* *Professor, School of Mechanical Engineering, Taiyuan University of Science and Technology, Taiyuan, Shanxi 030024, China.*
* *Key Laboratory of Intelligent Logistics Equipment in Shanxi Province, Taiyuan, Shanxi 030024, China.*
** *Graduate Student, School of Mechanical Engineering, Taiyuan University of Science and Technology, Taiyuan, Shanxi 030024, China.*

deviation using various methods. Hendrik Otto et al.(2019) the deviation of the conveyor belt when the idler moves laterally and the horizontal plane is deflected experimental setups, they constructed a lateral dynamics model to predict the deviation of the conveyor belt using stiffness matrix and deformation vector of the belt. Egger and Hoffman (2003) recorded deviation of the center line of the conveyor belt after the roller tilted using cameras. They observed that the conveyor belt immediately shifted as it approached the tilted pulley, and based on the beam bending theory, they used the second-order bending theory to calculate the lateral movement of the conveyor belt, indicating that the lateral movement of the belt was proportional to the angle of tilt of the pulley. YIN et al. (2020) used a MBD approach to discretize the conveyor belt and established a multi-body nonlinear contact dynamics model for the belt conveyor. They analyzed the monotone increasing relationship between the parallelism of the pulley and the deviation of the conveyor belt, showing that the greater the operating speed and distance of the conveyor belt, the larger degree of deviation. Zhang (2011) based on Euler-Bernoulli bending theory, divided the conveyor belt into free span sections and sections around the pulley, established the differential equations for the lateral movement of the belt, constructed a set of nonlinear equations, and solved it iteratively to obtain the relationship between the deflection angle of the pulley and the misalignment. Schmidrathner et al. (2022) using the finite element method, established a hybrid Euler-Lagrange lateral dynamics model to analyse the tangential and normal contact forces between the belt and the pulley during movement, parameterizing the lateral movement of the conveyor belt usings spatial coordinates. (BALAS et al. 1987; SIEVERS et al. 1988) treated the conveyor belt as a Timoshenko beam and analysed the deviation movement of a system composed of multiple segments of the conveyor belt. HAN et al. (2009) considered the inherent internal mechanical feedback of the annular flat belt and studied the deviation behavior of the conveyor belt with small lateral bending stiffness within the system ; Han et al. (2017) based on the quasi-static equation of Euler–Bernoulli beam, proposed a model to predict the lateral movement of the flat belt in relation to changes in the pulley's tilt angle over time, indicating that the flat belt tends to move toward the side with a shorter center distance, and the degree of misalignment increases with the increase of center distance and tension. Yoon et al. (2012) combined the finite element method and MDB to construct a shell element model of the conveyor belt with four nodes and proposed an efficient contact force search algorithm to analyse the deviation of the conveyor belt when the pulley is tilted, which was validated through experiments. Cheng et al. (2004) used the commercial finite element code MARC to propose a simulation method for analysing the deviation of the flat belt caused by the pulley deflection, examining the effects of deflection angle, tension and friction coefficient on the deviation of the belt.

Although many researchers have analysed the lateral movement of the belt using various methods and from different influencing factors, their research focus has primarily been on belt systems with only two pulleys. There has been less research on multi-pulley belt systems similar to belt storage units, and the lateral movement characteristics and influencing factors of multi-layer, multi-directional pulley belt systems within belt storage units remains unclear. Therefore, this paper establishes a lateral MBD model of the belt conveyor system within the belt storage units of the Telescopic Belt Conveyor. It analyses the belt deviation characteristics when there are in-plane and out-of-plane deflection angles present in the take-up pulleys, as well as the influence of the deflection angle of the take-up pulleys and the center distance H (distance between the bend pulley and the take-up pulley) of the pulleys on the deviation of the belt conveyor.

MODELLING METHOD

Introduction to MBD

MBD is the science that studies the motion laws of multi-body systems composed of multiple interconnected flexible or rigid objects. It mainly includes the dynamics of multi-rigid body systems and flexible systems (Liu, 2013). A system composed of multiple interconnected objects is referred to as a multi-body system. A multi-rigid body system consists of multiple rigid bodies, while a flexible system includes flexible bodies. Early research on multi-body systems employed classical mechanics methods, represented by vector mechanics methods such as the Newton-Euler equations and analytical mechanics methods represented by the Lagrange equations. To address the complex dynamics modeling of multi-body systems, researchers have combined classical mechanics methods with modern computational techniques, proposing various methods such as graph theory, variational methods, screw theory, and Kane's method. These methods can be categorized into relative coordinate methods and absolute coordinate methods.

The research object of MBD is a mechanical system where multiple rigid or flexible bodies are connected through joints or force elements. The fundamental equations of motion characterize the relationship between motion parameters and forces acting on the system. The relative coordinate method describes the system using the generalized coordinates of each joint, where the generalized coordinates typically represent the relative angles or displacements between the connected rigid or flexible

bodies. Thus, the system's position can be completely determined by the array of generalized coordinates of all joints. The differential equations of motion for multi-body systems using the relative coordinate can be expressed (Rong et al. 2011):

$$M(q,t)\ddot{q} = B \tag{1}$$

In the equation, $q,\ddot{q} \in R^n$ the symbols represent respectively the generalized coordinates of the system and their second derivatives with respect to time; $M \in R^{(n\times n)}$ is the system's generalized quality matrix; $B \in R^n$ is a generalized force vector.

positions and other motion quantities of the When modeling multi-body systems using the relative coordinate method, the number of equations is relatively small, making it more convenient and efficient for modeling and solving complex systems. By applying mathematical methods to solve the system of differential equations, one can obtain the moving objects.

The telescopic belt conveyor has both flexible and rigid components, and it includes a storage belt hopper structure, which adds complexity to the arrangement of the conveyor belt and the contact between the belt and the rollers and idlers. Therefore, using MBD methods can better analyze the deviation characteristics of the conveyor belt. The main moving components of the retractable belt conveyor include the conveyor belt, rollers, and idlers. Since the stiffness of the conveyor belt is much smaller than that of the rollers and idlers, the conveyor belt is treated as a viscoelastic flexible body, while the rollers and idlers are treated as rigid bodies. contact between the conveyor belt and the rollers and idlers is considered as a rigid-flexible coupling contact.

Discrete Modelling of Conveyor Belts

The conveyor belt model is based on the discrete modelling method of the Kelvin viscoelastic model, which discretizes the conveyor belt into rigid finite elements (RFE) with mass and inertia connected by spring-damping elements (SDE). After the conveyor belt is discretized into belt units, it can be regarded as a multi-body system with flexible connections. The nonlinear spring and damping parameters between adjacent rigid belt units are used to solve the nonlinearity of the conveyor belt material.

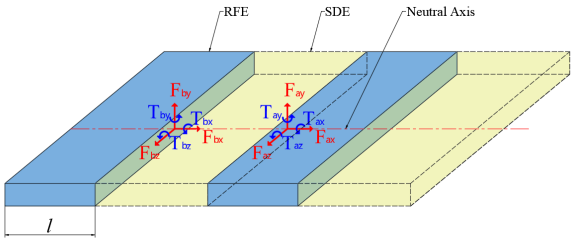

Fig. 2. Discrete model of conveyor belt.

The connecting force between adjacent belt units is related to the stiffness coefficient matrix and the damping coefficient matrix of the conveyor belt, which includes elastic forces and damping forces. In this paper, the connecting force between belt units are modeled using beam forces, defined based on Timoshenko beam theory, which represents the force and moment (as shown in Figure 2). The calculation Eq. is as follows (Liu, 2013):

$$\begin{bmatrix} F_{ax} \\ F_{ay} \\ F_{az} \\ T_{ax} \\ T_{ay} \\ T_{az} \end{bmatrix} = -\begin{bmatrix} K_{11} & & & & & \\ & K_{22} & & & & K_{26} \\ & & K_{33} & & K_{35} & \\ & & & K_{44} & & \\ & & K_{35} & & K_{55} & \\ & K_{26} & & & & K_{66} \end{bmatrix} \begin{bmatrix} l_x - l \\ l_y \\ l_z \\ \sigma_x \\ \sigma_y \\ \sigma_z \end{bmatrix} - \begin{bmatrix} C_{11} & C_{12} & C_{13} & C_{14} & C_{15} & C_{16} \\ C_{21} & C_{22} & C_{23} & C_{24} & C_{25} & C_{26} \\ C_{31} & C_{32} & C_{33} & C_{34} & C_{35} & C_{36} \\ C_{41} & C_{42} & C_{43} & C_{44} & C_{45} & C_{46} \\ C_{51} & C_{52} & C_{53} & C_{54} & C_{55} & C_{56} \\ C_{61} & C_{62} & C_{63} & C_{64} & C_{65} & C_{66} \end{bmatrix} \begin{bmatrix} V_x \\ V_y \\ V_z \\ \omega_x \\ \omega_y \\ \omega_z \end{bmatrix} \tag{2}$$

Among them, l_x, l_y, l_z, σ_x, σ_y, σ_z are the translational and rotational displacement of the moving marker relative to the base marker. V_x, V_y, V_z, ω_x, ω_y, ω_Z are the relative translational and rotational speed. K_{ij} the Eq. is as follows:

$$\begin{cases} K_{11} = \dfrac{E'A}{l} \\ K_{22} = \dfrac{12E'I_{xx}}{[l^3(1+P_y)]} \\ K_{33} = \dfrac{12E'I_{yy}}{[l^3(1+P_z)]} \\ K_{44} = \dfrac{GI_{xx}}{l} \\ K_{55} = \dfrac{(4+P_z)E'I_{yy}}{[l(1+P_z)]} \\ K_{66} = \dfrac{(4+P_y)E'I_{xx}}{[l(1+P_y)]} \\ K_{26} = \dfrac{-6E'I_{xx}}{[l^2(1+P_y)]} \\ K_{35} = \dfrac{-6E'I_{yy}}{[l^2(1+P_z)]} \end{cases} \tag{3}$$

of which,

$$\begin{cases} P_y = \dfrac{(12E'I_z zASY)}{(GAl^2)} \\ P_z = \dfrac{(12E'I_y yASZ)}{(GAl^2)} \end{cases} \tag{4}$$

where, E' is Young's modulus for conveyor belts (N/mm^2), which is the elastic modulus along the longitudinal direction with the value $E' = E/l$; A is Cross-sectional area of conveyor belt (mm^2); l is the Width of belt unit (mm); I_{xx}, I_{yy}, I_{zz} is the moment of inertia; ASY, ASZ are correction factors for shear deformation in the Y and Z directions with belts, $ASY = ASZ = 1.2$; G is the modulus of elasticity of the conveyor belt (N/mm^2).

The damping coefficient matrix is:

$$[C] = ratio \times [K] \tag{5}$$

where, $ratio$ is the damping coefficient, $[K]$ is the stiffness matrix.

Lateral MBD Modelling

Analysis of contact force

After the conveyor belt is discretized into several belt units, the continuous contact between the segments and the rollers and idlers essentially acts as a dynamic constraint, resulting in contact forces between the two contacting components (as shown in Figure 3). When the conveyor belt experiences lateral movement, the contact forces primarily consist of normal contact forces f_n, tangential friction forces f_{fl}, and lateral friction forces f_{f2}, with the contact between the belt units and the rollers and idlers being related to their own material properties.

The contact normal force f_n between the belt units and the pulleys and idlers arises from the tension of the belt units or the gravitational force acting at the contact points with the pulleys and idlers, directed along the normal direction of the contact point, always pointing toward the center of the pulleys or idlers. In rigid-flexible coupling contact, the normal contact force f_n can be viewed as a nonlinear spring connection relationship, modified based on Hertz contact theory, resulting in the normal contact force f_n being given by(□ □ □, 2009):

$$f_n = k\delta^{m1} + c\frac{\dot{\delta}}{|\dot{\delta}|}|\dot{\delta}|^{m2}\delta^{m3} \tag{6}$$

Where, k is spring coefficient; c is damping coefficient; δ and $\dot{\delta}$ are the penetration depth and the time derivative of the penetration depth, respectively; m_1, m_2, and m_3 are the spring exponents, damping exponents, and indentation exponents, respectively.

The belt conveyor operates on friction drive, and the power is transmitted through the tangential friction forces f_{fl} between the conveyor belt and the pulleys and idlers. When the conveyor belt undergoes lateral movement, the friction force between the belt and the rollers and idlers is primarily sliding friction f_{f2}. The calculation of the friction force between the conveyor belt and the rollers and idlers is as follows (Choi et al.2010):

$$f_{fi} = -sgn(v)\mu(v)\cdot|f_n| \tag{7}$$

$$\mu(v) = \begin{cases} havsin(v, 0, 0, v_s, \mu_s) & 0 \le |v| \le v_s \\ havsin(v, v_s, \mu_s, v_d, \mu_d) & |v| > v_s \end{cases} \tag{8}$$

Where f_n is the contact normal force; v is relative velocity; v_s, v_d are the static threshold velocity, dynamic threshold velocity, respectively; μ_s and μ_d are the static friction coefficient, dynamic friction coefficient, respectively.

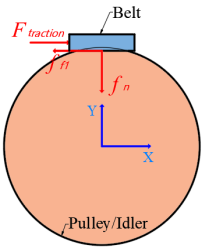

(a) contact normal force and tangential friction force

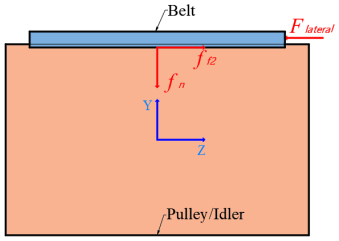

(b) contact normal force and lateral friction force

Fig. 3. Contact force between conveyor belt and pulley and idler.

Analysis of lateral restoring force

When the conveyor belt moves laterally, it experiences a force that opposes the lateral movement or a force that causes the conveyor belt to move in the opposite direction. The opposite movement of the conveyor belt is referred to as restore motion, and the force that prevents lateral motion or causes the conveyor belt to move in the opposite direction is termed the restore force.

(1) When the pulleys experiences an in-plane deflection angle β_H, the conveyor belt radius R_i of rotation along the width direction after entering the

pulley is inconsistent (as shown in Figure 4a), resulting in different tensions along the width of the belt F_{qi}. The larger the rotational radius R_i, the greater the tension F_{qi}, and this tension F_{qi} generates a lateral component F_{ZHi} in the direction of the larger rotational radius, causing the belt to move in that direction. This movement direction is opposite to the lateral motion direction of the conveyor belt caused by the roller's in-plane deflection angle. The restore force F_{ZHi} at each point along the width direction is expressed as:

$$F_{ZHi} = F_{qi} sin\beta_H \tag{9}$$

(2) When the misaligned conveyor belt is operating on the idler, it forms an angle θ with the idler (as shown in Figure 4b). The conveyor belt will experience a restore force F_Z due to the running resistance F_W of the idler, which acts along the axis of the idler and opposite to the direction of deviation. This can be expressed as:

$$F_z = F_w sin\theta \tag{10}$$

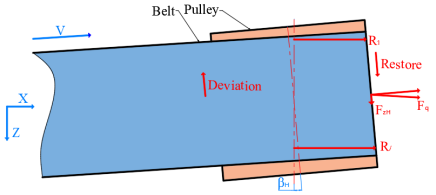

(a) Restore force of conveyor belt when passing through pulley

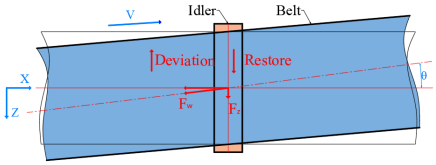

(b) Restore force of the conveyor belt as it passes through the idler

Fig. 4. Lateral restore force.

Simulation model establishment

RecurDyn (Recursive Dynamic) is a professional CAE software developed by the Korean company FunctionBay (FunctionBay Inc.) for MBD analysis. By using recursive equation based on relative coordinate systems, it efficiently performs dynamic modeling and analysis of both rigid and flexible multi-body systems.

In RecurDyn, a telescopic belt conveyor model is built using the Belt Toolkit. This paper focuses on the belt deviation characteristics within the belt storage units. To save simulation computation time, the length of the conveyor carrying section is shortened, while the belt storage units are modeled based on actual conditions, there is no material on the conveyor, and the grooved pulley in the bearing part is simplified to a flat pulley. It is assumed that the friction coefficient between the conveyor belt, pulleys and idlers is unchanged. The temperature and humidity of the underground coal mine environment are basically constant, and the influence of temperature and humidity changes on the performance of the conveyor belt is ignored. The main technical parameters of some key components are listed in Table1.

Table 1. Key component parameters for telescopic belt conveyor belt storage units.

Parameter	value	Parameter	value
Conveying capacity Q (t/h)	800	Diameter of bend pulley 1 (mm)	800
Conveying speed V (m/s)	3.5	Diameter of bend pulley 2 (mm)	630
Conveyor belt type	PVG1400S	Diameter of bend pulley 3 (mm)	1000
Width of belt B (mm)	800	Diameter of take-up pulley 1 (mm)	1000
Tension T (N)	13000	Diameter of take-up pulley 2 (mm)	630
Center distance H (m)	4~24	Diameter of take-up pulley 3 (mm)	800

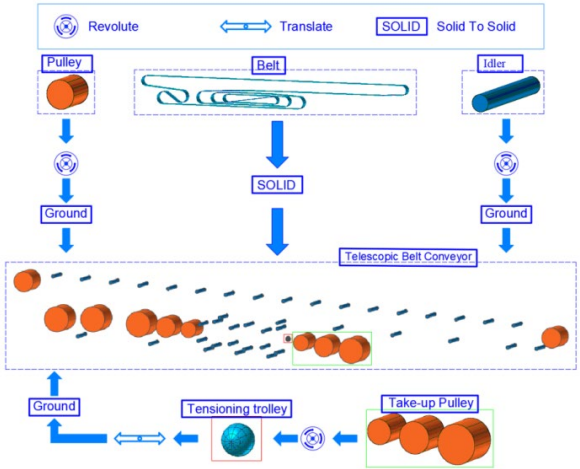

Fig. 5. Topology of the telescopic belt conveyor components.

According to the working principles of the telescopic belt conveyor, the relevant components are simplified: the supporting structures, such as the intermediate frame of the conveyor, are simplified, and the pulleys and support idlers are set with fixed coordinates in space; the drive device is simplified by implementing a circumferential drive function on the drive pulley; the tensioning device is simplified by establishing a translational joint between the take-up pulleys in the belt storage units and the ground, allowing for the tensioning of the belt. The topological structure of telescopic belt conveyor is shown in Figure 5.

The length of the belt units l is 62mm. The conveyor belt model is established using the Assembly entity modeling feature. The connection forces and moments between the belt blocks are created based on the Beam force model. Using the relevant parameters of the conveyor belt from Table 1, the stiffness matrix and damping matrix in the Beam force are calculated using Eq. (3) and (4). In RecurDyn software, the parameters k, c, δ, m_1, m_2, m_3 are set respectively, and the normal contact force f_n between the belt blocks and the pulleys and support idlers can be calculated using Eq. (6). Eq. (8) indicates that the friction coefficient between the belt and the pulleys and support idlers is determined by the relative velocity v and the threshold velocity v_s, v_d. Then, the friction force under different motion states is calculated using Eq. (7). The contact parameters (SUN et al.2024) between the conveyor belt and the pulleys and support idlers are shown in Table 2.

Table 2. Contact parameters between conveyor belt and pulley and idler.

Parameter	value	Parameter	value
Stiffness Coefficient k (N/mm)	2855	Static Threshold Velocity v_s (mm/s)	0.1
Damping Coefficient c ($N \cdot s/m$)	0.57	Stiffness Exponent m_1	1.1
Dynamic Friction Coefficient μ_d	0.3	Damping Exponent m_2	1.1
Dynamic Threshold Velocity v_d (mm/s)	10	Indentation Exponent m_3	1.1
Static Friction Coefficient μ_s	0.35	Penetration depth δ (mm)	0.1

According to the actual working conditions of the Telescopic Belt Conveyor, the conveyor drive system is a double-drum drive, and the tensioning system are three take-up pulleys at the end of the belt storage units that moves as a whole to tension the belt. The drive functions of the drive pulley and the take-up pulley are set, as shown in Table 3 and Table 4.

Table 3. Drive pulley drive function and tensioning drive function for different pulley center distances.

Parameter	value
Drive pulley 1	(-1)*IF(time-1:step(time,0,0,1,0),0,IF(time-8.0:0.42857143*(time-1)*(time-1)-0.04081633*(time-1)*(time-1)*(time-1),7,7))
Drive pulley 2	IF(time-1:step(time,0,0,1,0),0,IF(time-8.0:0.42857143*(time-1)*(time-1)-0.04081633*(time-1)*(time-1)*(time-1),7,7))

Table 4. Tensioning drive function for different pulley center distances.

Parameter	center distances H(mm)	value
Tensioning drive	4000	STEP(TIME,0,0,1,107)
	6000	STEP(TIME,0,0,1,100)
	8000	STEP(TIME,0,0,1,96)
	10000	STEP(TIME,0,0,1,90)

In Table 3, the driving functions for drive pulley 1 and drive pulley 2 are represented as angular velocity parameters, with the two drive pulleys rotating in opposite directions. The starting mode is a parabolic acceleration start, with an initial velocity of 0, reaching a rated velocity of 3.5m/s after 8s. In Table 4, the driving function of the take-up pulleys are represented as a displacement function, with the tensioning displacements set for center distances H=4000mm, H=6000mm, H=8000mm, and H=10000mm. The initial displacement is 0, and the tensioning displacement is achieved within 1s, reaching a rated tension of 13000N.

Another study on dynamic tension verified the simulation modeling method and contact parameters of the above conveyor, the results show that the simulation model tension is basically the same as the experimental tension (SUN et al.2024), which indicates the conveyor model and contact parameters are correct. Concurrently, the telescopic belt conveyor model established in this paper will not deviation of belt when the deflection angle of the take-up pulley is 0, which is consistent with the actual situation.

The simulation model of the telescopic belt conveyor is shown in Figure 6. The centroid of roller 3 is set as the coordinate origin. Based on the winding configuration of the conveyor belt within the belt storage units, the conveyor belt is divided into 9 segments:

Segment *ab*: from the separation point of Drive pulley 2 to the entrance point of take-up pulley 1.

Segment *bb'*: from the entrance point of take-up pulley 1 to the separation point.

Segment *b'c*: from the separation point of take-up pulley 1 to the separation point of bend pulley 1.

Segment *cd*: from the separation point of bend pulley 1 to the entrance point of take-up pulley 2.

Segment *dd'*: from the entrance point of take-up pulley 2 to the separation point.

Segment *d'e*: from the separation point of take-up pulley 2 to the separation point of bend pulley 2.

Segment *ef*.: from the separation point of bend pulley 2 to the entrance point of take-up pulley 3.

Segment *ff'*: from the entrance point of take-up pulley 3 to the separation point.

Segment *f'g*: from the separation point of take-up pulley 3 to the separation point of bend pulley3.

In Fig. 6, disp sensors are placed at the centroid points of take-up pulleys 1, 2, and 3 to measure the distance along the Z-axis between the centroid points of the take-up pulleys and the centroid points of the belt blocks, which represents the lateral displacement. Tension sensors are set on the conveyor belt at positions *ab*, *cd*, and *ef* to measure the tension at different locations on the belt. Belt unit 152, located at the separation point of Drive Roller 2, is designated as the operational output and force output unit to analyze the lateral movement characteristics

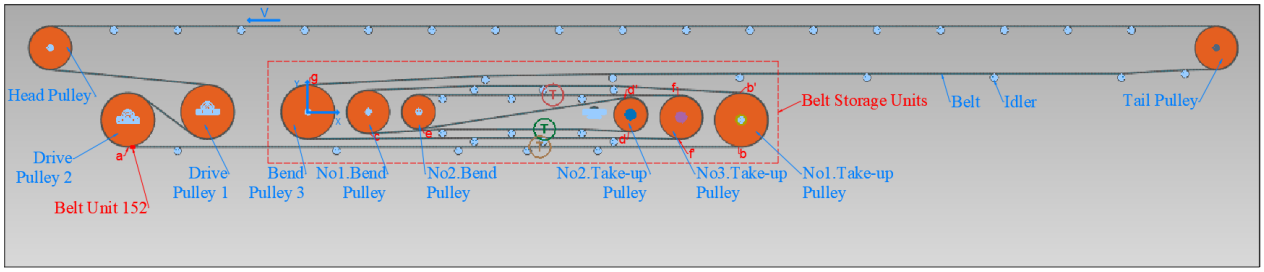

Fig. 6. Simulation model of the telescopic belt conveyor.

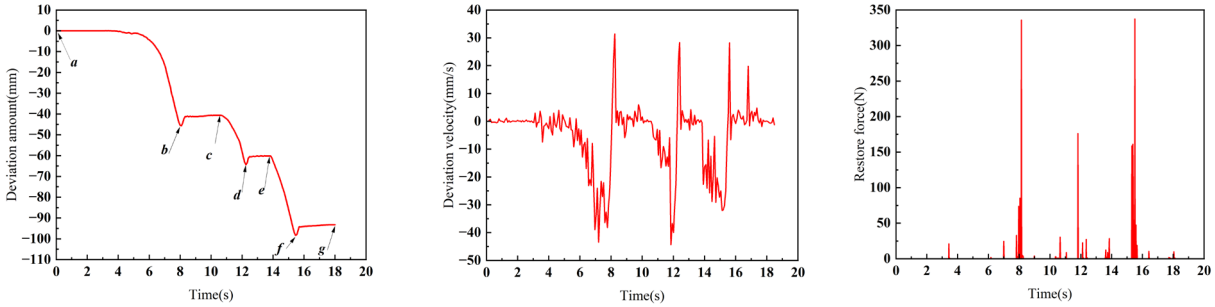

(a) Deviation amount (b) Deviation velocity (c) Restore force

Fig. 7. Deviation characteristics of belt unit 152 when the take-up pulley is in-plane deflection.

of the belt unit within the belt storage units. This setup allows for the collection of displacement, velocity, acceleration, and force exerted on the belt unit along the coordinate directions.

ANALYSIS OF BELT DEVIATION CHARACTERISTICS IN BELT STORAGE UNITS

This study uses the in-plane deflection angles β_H of the three take-up pulleys, the out-of-plane deflection angles β_V of the three take-up pulleys, and the center distance H between the bend pulley and the take-up pulley as experimental variables. Through simulation experiments, it evaluates the deviation, deviation velocity, and changes in tension of the conveyor belt as it passes around the deflected take-up pulleys within the belt storage units. The aim is to explore the influencing factors of belt deviation within the belt storage units and clarify the deviation characteristics of the storage belt units.

In-plane Deflection of the Take-up Pulley

Analysis of belt unit deviation

Taking belt unit 152 as the research subject, with set to H=4m, β_H=0.5°, the belt unit starts at point a, traveling through the belt storage units to reach point g, with a simulation time of 18s.

When analyzing the deviation characteristics of belt unit 152 in the time domain, we observe that the deviation undergoes three changes (Figure 7a) as the belt unit travels from point a through the belt storage units to point g and exits. Specifically, the deviation values are 45.52mm in segment ab, 23.75mm in segment cd, and 38.16mm in segment ef. Furthermore, the deviation in segment cd is based on the maximum deviation in segment ab, and the deviation in segment ef is based on the deviation in segment cd. Thus, we can conclude:

$$W_H = W_{ab} + W_{cd} + W_{ef} \tag{11}$$

in the equations:

W_H -is the total deviation of the belt unit as it passes through the belt storage units.

W_{ab} -is the deviation of the belt unit in segment ab.

W_{cd} - is the deviation of the belt unit in segment cd.

W_{ef} -is the deviation of the belt unit in segment ef.

During the three deviation processes, the deviation velocity of the belt unit gradually increases (Fig. 7b), with the maximum deviation velocity of 43.43mm/s in segment ab, 44.36mm/s in segment cd and 32.01mm/s in segment ef. In Fig. 7c, at points b, d, and f, where the belt unit enters take-up pulley 1, take-up pulley 2, and take-up pulley 3 respectively, it experiences a restoring force in the opposite direction of the deviation. The maximum restoring forces are 335.94N, 176.25N, and 337.35N, which continue to act on the belt unit until it exits the take-up pulleys. In Fig. 7a, it can be clearly seen that the deviation of the belt unit experiences a sudden change at points b, d, and f, with restoring displacements of 4.27mm, 3.79mm, and 4.16mm, respectively. The deviation

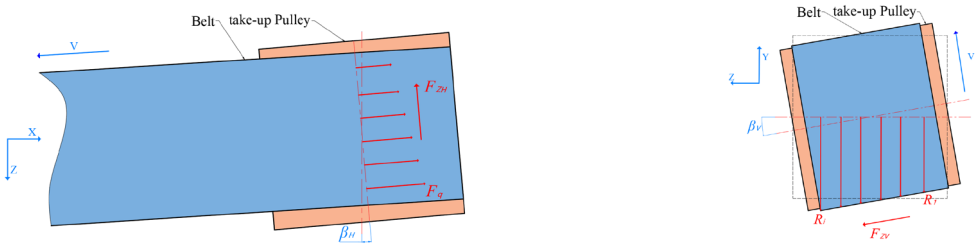

(a) In-plane deflection (b) Out-of-plane deflection

Fig.8. Lateral force caused by deflection of the of the take-up pulley

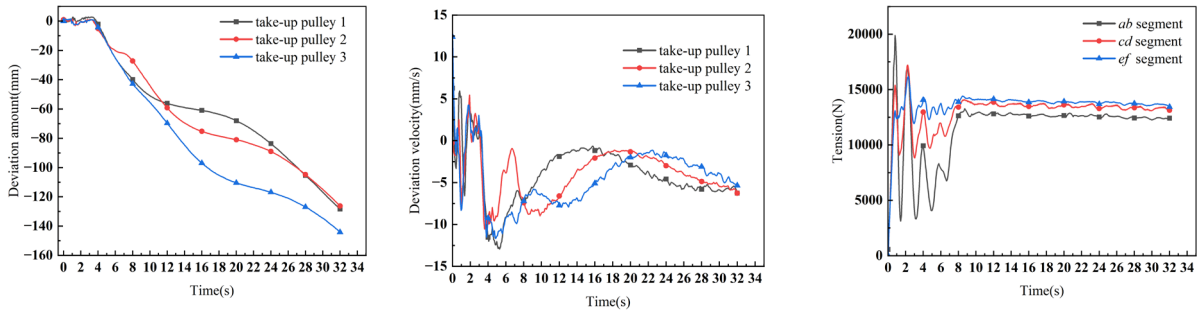

(a) Deviation amount (b) Deviation velocity (c) Conveyor belt tension

Fig. 9. Deviation and tension change at each take-up pulley when the in-plane deflection of the take-up pulleys deflects.

velocity of the belt unit decreases rapidly, approaching nearly 0 when it exits the take-up pulleys, consequently, there is no deviation in segments *bc*, *de*, and *fg*.

When the take-up pulley has an in-plane deflection angle β_H, the tension distribution of the conveyor belt entering the take-up pulley is inconsistent across its width. The tension decreases from the tight side to the slack side, resulting in a tension difference on both sides of the conveyor belt. This creates an axial lateral force F_{ZH} that causes the conveyor belt to deviate in the direction of reduced tension (see Figure 8a). As shown in Fig. 7a, the direction of the lateral force is only related to the deflection direction of the pulley and is independent of the running direction of the conveyor belt. Furthermore, the longer the running time of the belt unit before entering the take-up pulley, the greater the amount of deviation.

Analysis of belt deviation characteristics at the take-up pulleys

Taking the centroid points of the three take-up pulleys as observation references, the conveyor belt runs in a complete cycle of 32s from startup.

The deviation of the conveyor belt at the take-up pulleys gradually increases (Figure 9a), with the maximum deviation at take-up pulley 3 (segment *ef*) reaching 144.12mm. The maximum deviation at take-up pulleys 1 and 2 (segments *ab* and *cd*) are 128.35mm and 125.21mm, respectively. This indicates that when the take-up pulley has an in-plane deflection angle β_H, the deviation of the conveyor belt at take-up pulley 3 is the largest in the belt storage units.

From Fig. 9b, it can be observed that during the 0-8s, the conveyor is in the startup phase, and the deviation velocity of the conveyor belt at the three rollers gradually increases. The conveyor belt starts operating at 1 second, showing significant fluctuations in deviation velocity, reaching a maximum deviation velocity of 12mm/s at 4s. After 4s, the deviation velocity gradually decreases, and at 8s, the conveyor achieves its rated belt velocity. The deviation velocity at take-up pulley 1 decreases to 0.9mm/s at 15s, then gradually increases, stabilizing around 6mm/s during the period from 26-32s. At take-up pulley 2, the deviation velocity decreases to 1.12mm/s at 18.5s, then gradually increases, reaching 5.8mm/s at 32s. At take-up pulley 3, the deviation velocity reduces to 1.08mm/s at 23s and then gradually increases, reaching 5.57mm/s at 32s. From 8-20s, the deviation velocity at take-up pulley 3 is greater than that at take-up pulley 1 and 2, and it takes only 12s for the deviation velocity to increase to a level comparable to that at take-up pulley 1 and 2.

In Fig. 9c, the tension of the conveyor belt at the three deviation points within the belt storage units shows significant fluctuations during the startup phase of 0-8s. After 8s, the tension stabilizes, and tension in segment *ab* < tension in segment *cd* < tension in segment *ef*.

Out-of-plane Deflection of the Take-up Pulley

Analysis of belt unit deviation

Taking belt unit 152 as the research subject, with set to H=4m, β_V=0.5°, with a simulation time of 18s.

The deviation of belt unit 152 is analyzed in the time domain (Figure 10a). The deviation from point b to point b' is 9.55mm. The deviation from point d to point d' is 5.46mm, while the deviation from point f to point f' is 7.1mm. Notably, the deviation in segment dd' is based on the deviation in segment bb', and similarly, the deviation in segment ff' is based on the deviation in segment dd'. It is also evident that the direction of deviation at take-up pulley 3 is opposite to those at take-up pulleys 1 and 2. Therefore, when there is an out-of-plane deflection at the take-up pulleys, the belt unit experiences deviation upon entering the deflected roller, which disappears after exiting the roller. The total deviation the belt unit experiences while passing through the belt storage units is given by:

$$W_V = W_{bb'} + W_{dd'} - W_{ff'} \tag{12}$$

where,

W_V is the total deviation of the belt unit as it passes through the belt storage units;

$W_{bb'}$ -is the deviation of the belt unit at take-up pulley 1;

$W_{dd'}$ -is the deviation of the belt unit at take-up pulley 2;

$W_{ff'}$ -is the deviation of the belt unit at take-up pulley 3.

In Fig. 10b, when the belt unit enters take-up pulleys 1, 2, and 3, its deviation velocity suddenly changes within a very short time frame. Approximately within 0.4 seconds, the deviation velocity rapidly rises from 0 to 30mm/s and then quickly drops back to 0. The maximum deviation velocity during the three deviation events is 30.79mm/s, 29.94mm/s, and 29.96mm/s, respectively, which are nearly equal. In Fig. 10c, analyzing in conjunction with Fig.10a, the restoring forces at points d and f are 60.67N and 39N, respectively. It can also be seen from Fig. 10a that there are restoring effects just before reaching point d and in the $f'g$ segment.

When the take-up pulley has a deflection angle β_V in the out-of-plane, the rotational radius of the conveyor belt that enters the take-up pulley is inconsistent across its width. This variation in rotational radius creates a lateral force F_{ZV} in the direction of the increasing rotational radius, causing the conveyor belt to deviate (see Fig. 8b). Once the conveyor belt exits the take-up pulley, the lateral force F_{ZV} disappears, which means that the conveyor belt will not actively deviate at other locations, and the direction of the deviation is related to the direction in which the conveyor belt enters the pulley. As indicated by the deviation amounts of the belt unit on each take-up pulley in Fig. 10a, the amount of deviation is related to the diameter of the pulley; specifically, a larger diameter results in a greater deviation.

Analysis of belt deviation characteristics at take-up pulleys

Taking the centroid points of the take-up pulleys as observation references, the conveyor belt operates in a complete cycle of 32s.

At 3s, there is a significant deviation of the conveyor belt at take-up pulley 1 (Figure 11a), at which point the deviation velocity suddenly rises to 12.84mm/s, and subsequently decreases rapidly (Fig. 11b). From 4s-24s, there is basically no deviation, but after 24s, the deviation gradually increases. At take-up pulley 2, the deviation and deviation velocity gradually increase from 6s-13s, reaching a maximum deviation velocity of 4.28mm/s, after which both the deviation and velocity gradually decline. After 26s, the deviation begins to increase again. The presence of take-up pulley 3 causes the conveyor belt to misalign in the opposite direction, resulting in a smaller deviation compared to take-up pulley 2, and a restoring phenomenon occurs.

In Fig. 11a, the maximum deviation amounts at take-up pulleys 1, 2, and 3 are 8.01mm, 12.02mm, and 10.27mm, respectively. This indicates that when there is an out-of-plane deflection angle at the take-up pulleys, the deviation at take-up pulley 2 is the largest. Furthermore, the deviation and deviation velocity of the conveyor belt are significantly smaller when compared to scenarios where the rollers have an in-plane deflection angle.

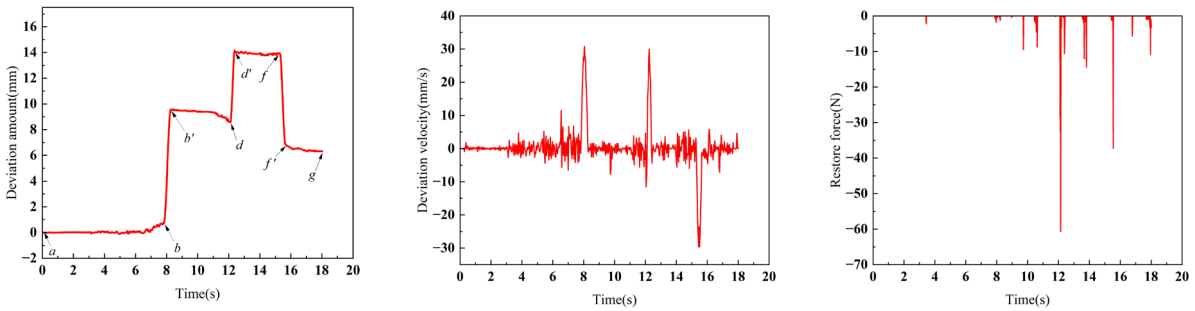

(a) Deviation amount (b) Deviation velocity (c) Restore force

Fig. 10. Deviation characteristics of belt unit 152 when the take-up pulley is in-plane deflection.

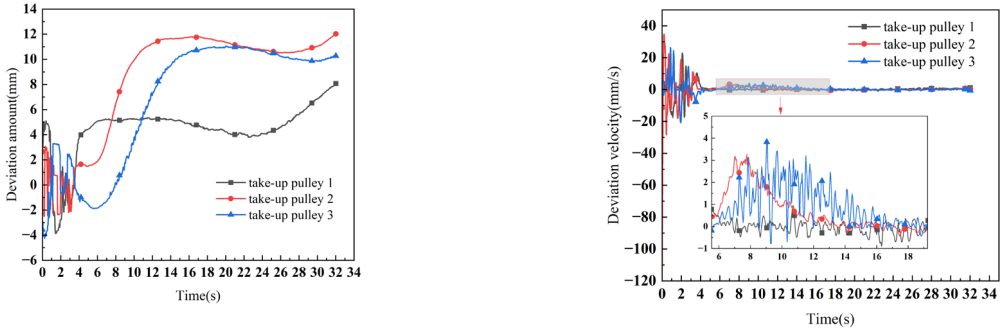

(a) deviation amount (b) deviation velocity

Fig. 11. Deviation characteristics at each take-up pulley when the take-up pulleys are out-of-plane deflection.

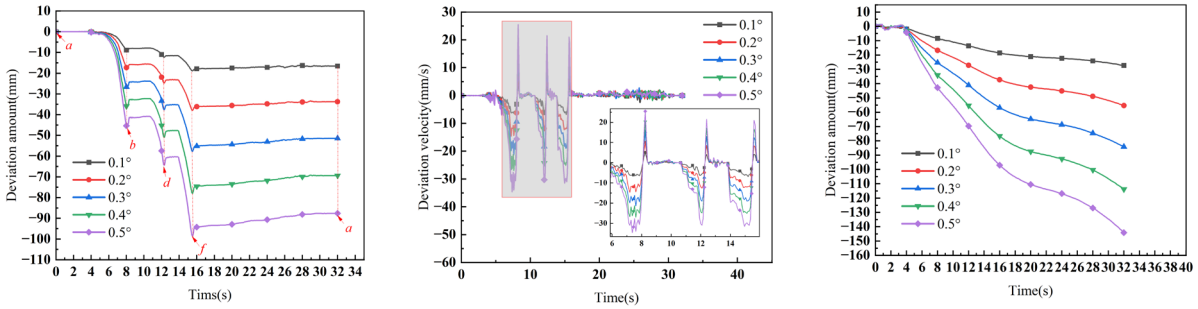

(a) Deviation amount of belt unit 152 (b) Deviation velocity of belt unit 152 (c) Deviation amount of conveyor belt at take-up pulley 3

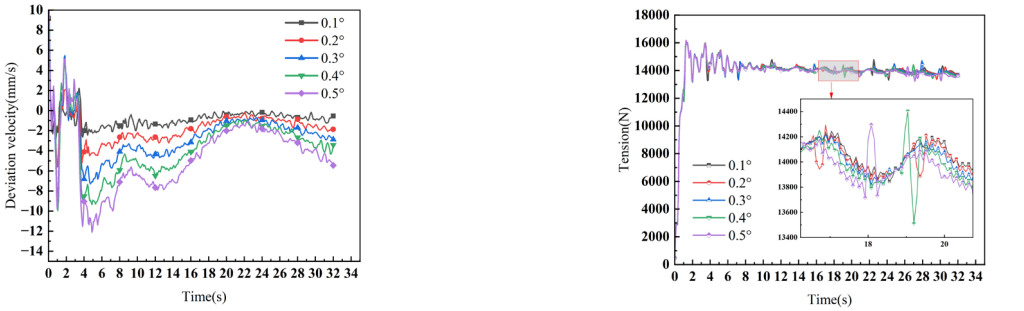

(d) Deviation velocity of conveyor belt at take-up pulley3 (e) Conveyor belt tension in the *ef* segment

Fig. 12. Deviation characteristics and tension change of conveyor belt at different in-plane deflection angles.

Impact of Pulley In-plane Deflection Angle on Deviation

Taking belt unit 152 and take-up pulley 3 as the subjects of study, with set to H=4000mm and the in-plane deflection angle β_H as the experimental variable, belt unit 152 is simulated to start from point a, complete one cycle, and return to point a, with a total simulation time of 32 seconds. The deviation characteristics of the conveyor belt are analyzed during this period when β_H=0.1°, β_H=0.2°, β_H=0.3°, β_H=0.4°, β_H=0.5°.

As the in-plane deflection angle β_H of the take-up pulley gradually increases, the deviation quantity of belt unit 152 within the belt storage units also increases progressively (Figure 12a). With the in-plane deflection angle β_H increasing from 0°to 0.5°, As demonstrated in Table 6, an increase in deflection angle of 0.1° is associated with a corresponding deviation in the belt unit at 32s. At points *b*, *d*, and *f*, the restoring quantity of the belt unit also increases with the increase in the in-plane deflection angle (Fig. 12a). When the belt unit leaves point *g* and enters the return section and load-carrying section, it then returns to point *a*, the restoring phenomenon occurs in segment *fa* of the conveyor belt, and the restoring quantity will also increase with the growing in-plane deflection angle β_H (Table5). The velocity of deviation and the restoring velocity of the block accelerate as the in-plane deflection angle β_H increases (Fig. 12b).

Table 5. Restoring quantity of conveyor belt in the *fa* segment.

β_H (°)	0.1	0.2	0.3	0.4	0.5
Restoring amount (mm)	8.7	18.04	27.29	37.13	47.18

In Fig. 12c and 12d, when the conveyor belt is running for 32s, the deviation amount and velocity of the conveyor belt at take-up pulley 3 (segment *ef*) increase with the in-plane deflection angle β_H (Table6). Additionally, the tension of the conveyor belt in segment *ef* decreases as the in-plane deflection angle β_H increases (Fig. 12e). This is because the increase in the in-plane deflection angle β_H amplifies the tension difference on both sides of the conveyor belt, resulting in a larger lateral force F_{ZH} generated by this tension difference. For every increase of 0.1° in the deflection angle β_H, the average increment in the deviation amount at the take-up pulley 3 is 17.53mm. Therefore, the deviation amount $W_{H(n)}$ of the conveyor belt at the 3rd take-up pulley when the in-plane deflection angle β_H is given can be expressed as:

$$W_{H(n)} = \frac{\beta_{H(n)}}{\beta_{H(0.1)}}(W_{H1} + C_H) \quad n \geqslant 0.2 \qquad (13)$$

where, $W_{H1}$is the deviation quantity at take-up pulley 3 when β_H=0.1°; $\beta_{H(0.1)}$ is β_H=0.1°; C_H is the compensation coefficient, taken as 2.6.

Table 6. Belt deviation after 32 seconds of operation for belt unit 152 and take-up pulley 3.

β_H (°)	0.1	0.2	0.3	0.4	0.5
belt unit 152 (mm)	-16.5	-33.78	-51.41	-69.41	-87.63
take-up pulley 3 (mm)	-27.28	-55.34	-84.14	-113.79	-144.12

Impact of Pulley Out-of-plane Deflection Angle on Deviation

Taking belt unit 152 and take-up pulley 2 as the subjects of study, with set to *H*=4000mm and the out-of-plane deflection angle β_V as the experimental variable, belt unit 152 is simulated to start from point *a*, complete one cycle, and return to point *a*, with a total simulation time of 32s. The deviation characteristics of the conveyor belt are analyzed during this period when β_V=0.1°, β_V=0.2°, β_V=0.3°, β_V=0.4°, β_V=0.5°.

As the deflection angle β_V of the pulley increases, the difference in radius of rotation in the direction of the belt width also increases, so the lateral force F_{ZV} in the direction of the increasing radius increases. In Figure 13a, as the deflection angle β_V of the take-up pulley in the out-of-plane increases from 0.1°to 0.5°, the deviation of belt unit 152 in segments *bb'*, *dd'*, and *ff'* also increases correspondingly, the amount of deviation at 32s with the belt unit is shown in Table 7. The belt unit also exhibits a restoring phenomenon in segment *f'a* (Fig. 13a), with the restoring amount gradually increasing with the deflection angle (Table 8). The deviation velocity of the belt unit in segments *bb'*, *dd'*, and *ff'* also accelerate with the increase in the out-of-plane deflection angle (Fig. 13b), while in the other segments, the deviation velocity is basically 0.

As demonstrated in Figure 13c, after 32s, the deviation amounts at the take-up pulley 2 under different deflection angles β_V are shown in Table 7. For every increase of 0.1° in the deflection angle β_V, the average increment in the deviation amount at the take-up pulley 2 is 2.4 mm. Similarly, we can derive that when the out-of-plane deflection angle $\beta_{V(n)}$ is given, the deviation amount $W_{V(n)}$ of the conveyor belt at the take-up pulley 2 can be expressed as:

$$W_{V(n)} = \frac{\beta_{V(n)}}{\beta_{V(0.1)}}(W_{V1} + C_V) \quad n \geqslant 0.2 \qquad (14)$$

where, W_{V1} is the deviation quantity at take-up pulley 2 when β_V=0.1°; $\beta_{V(0.1)}$is β_V=0.1° ; C_V is the compensation coefficient, taken as 0.7.

Table 7. Belt deviation after 32 seconds of operation for belt unit 152 and take-up pulley 2.

β_H (°)	0.1	0.2	0.3	0.4	0.5
belt unit 152 (mm)	1.07	2.01	2.93	3.95	4.72
take-up pulley 2 (mm)	2.24	5.04	7.43	9.95	12.02

Table 8. Restoring amount of conveyor belt in the *fa* segment.

β_V (°)	0.1	0.2	0.3	0.4	0.5
Restoring amount (mm)	0.18	0.51	0.9	1.21	1.82

The deviation velocity of the conveyor belt begins to increase at 5s (Fig. 13d), reaching a maximum at 8s, with higher deflection angles β_V resulting in greater deviation velocity. After 8s, the velocity decreases.

Influence of Different Center Distances on Deviation

To investigate the effect of changes in the center distance *H* of the belt storage units after the belt is retracted and extended on deviation, belt units and take-up pulleys are taken as the subjects of study. The analysis is conducted on the deviation characteristics of the conveyor belt under conditions of in-plane and out-of-plane deflection angles β_H and β_V.

(1) In-plane deflection angle β_H present at the take-up pulley

With the in-plane deflection angle set at β_H=0.5°, the center distance *H* is treated as the experimental variable. belt unit 152 is simulated to start from point *a*, complete one cycle, and return to point *a*, with a total simulation time of 32s. The deviation characteristics of the conveyor belt are analyzed during this period at *H*=4000mm, *H*=6000mm, *H*=8000mm and *H*=10000mm respectively.

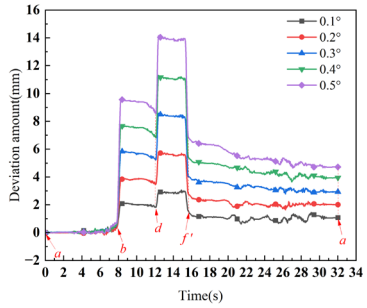

(a) Deviation amount of belt unit 152

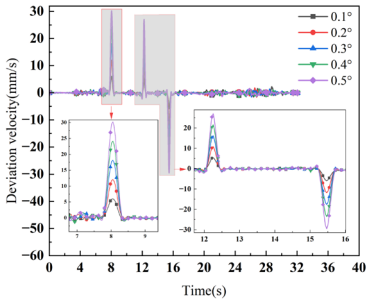

(b) Deviation velocity of belt unit 152

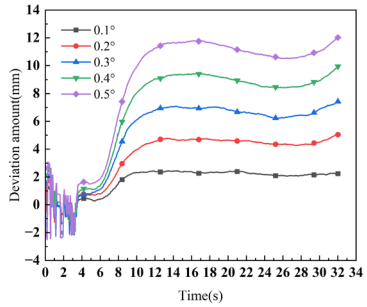

(c) Deviation amount of conveyor belt at take-up pulley 2

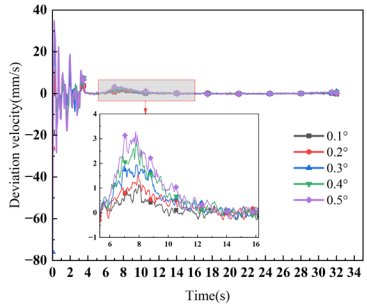

(d) Deviation velocity of conveyor belt at take-up pulley 2

Fig. 13. Deviation characteristics of conveyor belt at different out-of-plane deflection angles.

In Figure 14a, as the center distance H increases, the deviation of belt unit 152 in segments *ab*, *cd*, and *ef* also increases correspondingly. Due to the increase in H, the lengths of segments *ab*, *cd*, and *ef* become longer, causing the starting points of deviation at points *c* and *e* to be gradually delayed. Similarly, the ending points of deviation at points *b*, *d* and *f* are also delayed. However, the restoring amount in segment *fa* decreases as the center distance H increases (Table 9). In Fig. 14b, the deviation speeds of the belt unit in sections *ab*, *cd*, and *ef* are nearly equal, indicating that the deviation speed of the belt unit is not affected by the change in center distance H. Therefore, the reason for the increase in deviation amounts in each segment is that the running time of the belt unit has increased, resulting in a longer duration during which the belt unit are subjected to the lateral forces causing deviation.

Table 9. Restoring amount of conveyor belt in the *fa* segment.

Center distance H (mm)	4000	6000	8000	10000
Restoring amount (mm)	6.6	4.67	1.72	0.68

In Fig.14c, the deviation amount of the conveyor belt at the take-up pulley 3 increases as the center distance H increases. The deviation amounts at the take-up pulley 3 after the conveyor runs for 32s under different center distances H are shown in Table 10. From the increments in the deviation amounts, it can be observed that the variation in deviation amounts has a nonlinear relationship with the changes in H.

At the same time, the deviation velocity of the conveyor belt also increases correspondingly (Fig. 14d). However, as the center distance H increases, the trend of change in the deviation velocity decreases, indicating that the deviation velocity stabilizes at a more consistent value.

Table 10. Deviation of the take-up pulley 3 with different center distances H.

Center distance H (mm)	4000	6000	8000	10000
Deviation amount (mm)	144.12	171.89	183.98	215.88

(2) Out-of-plane deflection angle β_V present at the take-up pulley

With the out-of-plane deflection angle set at β_V =0.5°, the center distance H is treated as the experimental variable. belt unit 152 is simulated to start from point *a*, complete one cycle, and return to point *a*, with a total simulation time of 32s. The deviation characteristics of the conveyor belt are analyzed during this period at H=4000mm, H=6000mm, H=8000mm and H=10000mm respectively.

When the take-up pulley has an out-of-plane deflection angle β_V, as the center distance H increases, the deviation of belt unit 152 also increases accordingly (Figure 15a). However, the increase in center distance H has a minor effect on the change in deviation amount, and the difference in deviation of the belt unit on the three take-up pulleys being approximately 1mm. The change in restoring amount is similar to that when the roller has an in-plane deflection angle, where the restoring amount in segment *fa* decreases as the center distance H increases (Table 11). In Fig. 15b, it can be observed that the deviation velocity of the block in segments

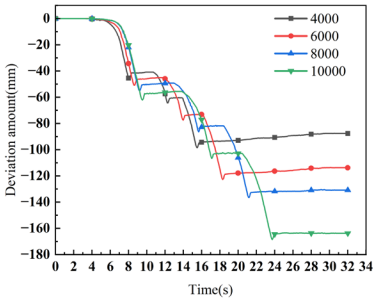

(a) Deviation amount of belt unit 152

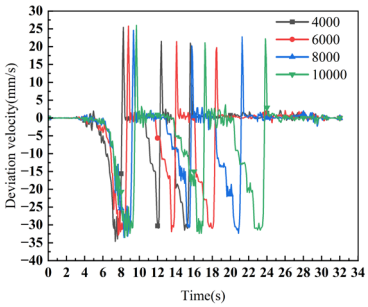

(b) Deviation velocity of belt unit 152

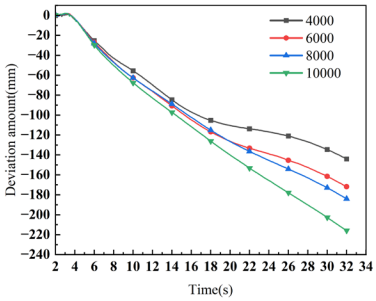

(c) Deviation amount of conveyor belt at take-up pulley 3

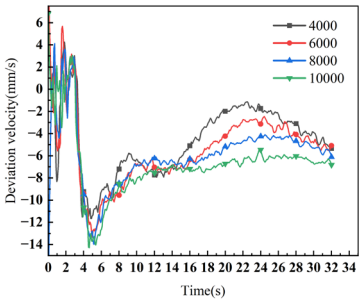

(d) Deviation velocity of conveyor belt at take-up pulley3

Fig. 14. Deviation characteristics of conveyor belt at different center distances *H* with an in-plane deflection angle of the take-up pulleys.

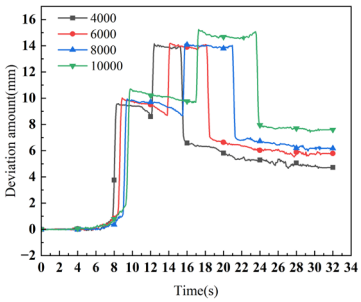

(a) Deviation amount of belt unit 152

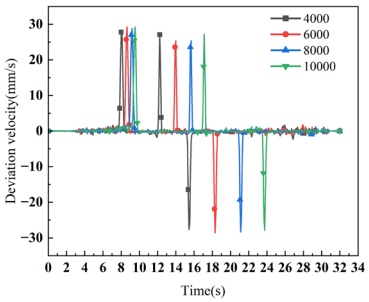

(b) Deviation velocity of belt unit 152

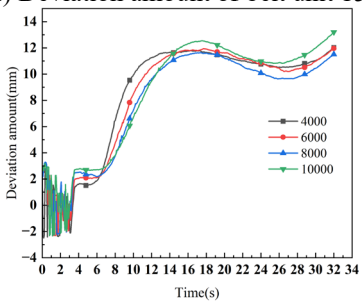

(c) Deviation amount of conveyor belt at take-up pulley 2

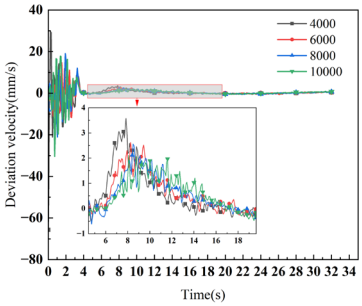

(d) Deviation velocity of conveyor belt at take-up pulley 2

Fig. 15. Deviation characteristics of conveyor belt with different center distances *H* for the take-up pulleys with out-of-plane deflection.

bb', *dd'*, and *ff'* is almost unaffected by changes in the center distance, and the deviation velocity in the same segments are generally consistent.

Table 11. Restoring amount of conveyor belt in the *fa* segment.

Center distance *H* (mm)	4000	6000	8000	10000
Restoring amount (mm)	1.87	1.11	0.64	0.22

In Fig.15c, the variation of the center distance *H* has a minor effect on the change in deviation amounts.

After the conveyor runs for 32s, the deviation amounts at the take-up pulley 2 under different center distances are shown in Table 12, with the difference in deviation amounts being less than 1.5 mm.

Additionally, 8s before, the deviation speed of the conveyor belt decreases with the increase in center distance H (see Fig.15d). After 8s, when the conveyor belt reaches its rated running speed, the deviation speeds gradually decrease and tend to converge to similar values. From the previous analysis, it can be concluded that the deviation of the conveyor belt occurs at the take-up pulleys, and the change in center distance H does not affect the belt's operation on the pulleys. Therefore, when the take-up pulley experiences a deflection in the out-of-plane, the deviation of the conveyor belt is almost unaffected by the change in center distance H.

Table 12. Deviation of the take-up pulley 2 with different center distances H.

Center distance H (mm)	4000	6000	8000	10000
Deviation amount (mm)	12.02	11.96	11.51	13.20

CONCLUSION

This paper analyzes the discretization modeling method of the conveyor belt in the belt storage units, the contact forces between the conveyor belt and pulleys, as well as the lateral restoring forces. It employs RecurDyn to establish a lateral multi-body dynamic model of the telescopic belt conveyor belt storage system and explores the deviation characteristics of the conveyor belt when the take-up pulley experiences in-plane and out-of-plane deflection in the belt storage units. The relationships between the in-plane deflection angle β_H, out-of-plane deflection angle β_V, and pulley center distance H and their effects on conveyor belt deviation within the belt storage units are revealed. The main conclusions are as follows:

1. When there is an in-plane deflection angle β_H at the take-up pulley in the belt storage units, the deviation of the conveyor belt is quite serious. In the direction of the conveyor belt's operation, deviation occurs as the belt approaches the front of the take-up pulley. The number of deviations times of the conveyor belt matches the number of take-up pulleys, and the directions of deviation are consistent. Consequently, the deviation quantities of the conveyor belt gradually accumulate, with the maximum deviation W_H in the belt storage units occurring at take-up pulley 3. Therefore, when implementing corresponding corrective measures, the corrective actions at take-up pulley 3 should be larger.

2. When there is an out-of-plane deflection angle β_V at the take-up pulley in the belt storage units, the deviation of the conveyor belt is relatively slight. In the direction of the conveyor belt's operation, deviation occurs as the belt wraps around the take-up pulley. The number of deviations corresponds to the number of take-up pulleys. The deviation direction is consistent on pulleys rotating in the same direction, while it is opposite on pulleys that rotate in the reverse direction. The position of maximum deviation W_V is at take-up pulley 2. Therefore, the corrective actions at take-up pulley 2 should also be larger.

3. The angle of deflection of the take-up pulley and the pulley center distance H are positively correlated with the deviation quantity of the conveyor belt. During the installation and use of the telescopic belt conveyor, efforts should be made to ensure the perpendicularity of the take-up pulley's axis to the conveyor's center-line and its parallelism with the plane of the conveyor belt, especially when the pulley center distance H is large. It is important to prevent the take-up pulley from having an inclination in either the in-plane or out-of-plane.

4. The deviation of the conveyor belt following a displacement is affected by the restoring force, which induces a restoring phenomenon and reduces the deviation quantity. The greater the number of support idlers encountered after leaving the belt storage units, the larger the restoring quantity of the conveyor belt.

5. When monitoring the deviation of the conveyor belt in the belt storage units, the focus should be on monitoring the take-up pulley 2 and take-up pulley 3. When designing the deviation correction device, as the number of deviations times of the conveyor belt within the belt storage units is related to the number of take-up pulleys, and since the deviation quantity varies at each take-up pulley, the number of corrective devices in the belt storage units should match the number of take-up pulleys. These corrective devices should be installed close to the take-up pulleys, with each corrective device providing different corrective force.

ACKNOWLEDGMENTS

This work was partially supported by the Shanxi Province Basic Research Program Joint Funding Project (Grant No. TZLH20230818015), and Taiyuan City's 'Top Ranking' Project for Tackling Key and Core Technologies (Grant No. 2024TYJB0117).

DECLARATIONS CONFLICT OF INTEREST

The authors declare no competing interests.

REFERENCES

BALAS, MARK, and ANDREAS VON FLOTOW, "Modeling of Web-Roller Interactions and Lateral Web Dynamics," *28th Structures, Structural Dynamics and Materials Conference*, pp.820 (1987).

Cheng, H., K Yoshida, and S Yanabe, “Finite Element Analysis of Belt Skew Caused by Angular Misalignment of Rollers,” *Proceedings of the Institution of Mechanical Engineers, Part C: Journal of Mechanical Engineering Science*, Vol. 218, No. 10, pp. 1223–32 (2004).

Choi, Juhwan, Han Sik Ryu, Chang, Wan Kim, and Jin Hwan Choi, “An Efficient and Robust Contact Algorithm for a Compliant Contact Force Model between Bodies of Complex Geometry,” *Multibody System Dynamics*, Vol. 23, No. 1, pp. 99–120(2010).

Egger, Martin, Anton Pirko, and Klaus Hoffmann, “Simulation of Flat Belt Running,” *Steel Research International*, Vol. 78, No. 4, pp. 364–68 (2007).

Hoffmann, Klaus, “Measurements and Simulation of Guiding Effects with Flat Belt Conveyors,” *XVII IMEKO World Congress, Metrology in the 3rd Millenium*, (2003).

Hoffmann, K, and M Egger, “Lateral Running Behavior of Conveyor Belt,” *Bulk Solids Handling*, Vol. 21, No. 3, pp. 301–6 (2001)

Han, F. L., Xiong F., Yi, P. X., and Shi, T. L, “Axial Motion of Flat Belt Induced by Angular Misalignment of Rollers,” in *2009 International Conference on Mechatronics and Automation*, pp. 3298–3303 (2009).

Han, F. L., He, R. B., Yan Hongzhi, and Xiong Feng, “Lateral Motion of the Endless Flat Belt in a Two-Pulley Belt System,” *Advances in Mechanical Engineering*, Vol. 9, No. 4, pp. 1687814017695955 (2017).

L. Sievers, M. J. Balas, and A. von Flotow, “Modeling of Web Conveyance Systems for Multivariable Control,” *IEEE Transactions on Automatic Control*, Vol. 33, No. 6, pp. 524–31 (1988).

Liu, Y., “*Basic Application and Improvement of Recurdyn Multibody Dynamics Simulation*,” Electronic Industry Press, Beijing (2013)

Otto, Hendrik, and André Katterfeld, “ Belt Mistracking - Simulation and Measurements of Belt Sideways Dynamics,” *University of Magdeburg, Chair of Material Handling Universitätsplatz*, Vol. 2, pp. 39104 (2019).

Rong, Bao, Xiao-ting Rui, Guo-Ping Wang, and Fu-feng Yang, “Developments of Studies on Multibody System Dynamics,” *Zhendong Yu Chongji (Journal of Vibration and Shock)*, Vol. 30, No. 7, pp. 178–87 (2011).

Schmidrathner, Christian, Yury Vetyukov, and Jakob Scheidl, “Non-Material Finite Element Rod Model for the Lateral Run-off in a Two-Pulley Belt Drive,” *ZAMM - Journal of Applied Mathematics and Mechanics / Zeitschrift Für Angewandte Mathematik Und Mechanik*, Vol. 102, No. 1, pp. e202100135 (2022).

SUN, X. X, XIAO, H, and MENG, W. J, “Dynamics Modeling and Simulation of Steel Cord Conveyor Belt Based on Dynamic Elastic Modulus,” *PROCEEDINGS OF THE INSTITUTION OF MECHANICAL ENGINEERS PART C-JOURNAL OF MECHANICAL ENGINEERING SCIENCE*, Vol. 238, No. 14, pp. 6910–22(2024).

YIN, Z. M., and FAN, Z. M., “Study on Deviation of Conveyor Belt Based on Multi-Body Dynamics Characteristics,” *Journal of Mechanical Engineering*, Vol. 56, No. 1, pp. 37–46 (2020).

Yoon, J S, J H Choi, T Suzuki, and J H Choi, “Numerical and Experimental Analysis for the Skew Phenomena on the Flexible Belt and Roller Contact Systems,” *Proceedings of the Institution of Mechanical Engineers, Part C: Journal of Mechanical Engineering Science*, Vol. 226, No. 5, pp. 1365–81 (2012).

Zhang, W. M., “Analysis on Skew of Flat Belts in Two-Pulley Drives,” *Journal of Mechanical Design*, Vol. 133, No. 111001 (2011).

□ □ □, “(A) Study on the Analysis of Rigid and Flexible Body Dynamics with Contact”, □ □ □ □ □ □ □ □, (2009).